INSTITUT NATIONAL DE RECHERCHE EN INFORMATIQUE ET EN AUTOMATIQUE

Superposition of Planar Voronoi Tessellations

François Baccelli — Catherine Gloaguen — Sergei Zuyev

N° ????

Mai 1999

THÈME 1

Rapport de recherche

ISSN 0249-6399

Superposition of Planar Voronoi Tessellations

François Baccelli[*] , Catherine Gloaguen[†] , Sergei Zuyev[‡]

Thème 1 — Réseaux et systèmes
Projet MISTRAL

Rapport de recherche n° ???? — Mai 1999 — 29 pages

Abstract: We study the tessellation defined as the intersection of two independent planar Poisson-Voronoi tessellations and derive the means of its main geometrical characteristics. For this intersection tessellation, we distinguish between six types of cells depending on whether they contain the nuclei of the two initial tessellations or not. The intensity and the mean area of each type of cell are computed either in closed form or via asymptotic expansions. The model can be used to represent the local zones of two competing telecommunication operators. Then the interconnection of two subscribers induces a specific cost within each type of cell of the intersection tessellation associated with the two systems of local zones.

OR/MS Subject Classification: Probability: stochastic model applications; Networks/graphs: stochastic; Communications; Transportation: network models.
AMS 1991 Subject Classification Primary : 60D05, 90B12, 93A13
Secondary : 60G09, 60G10, 60K99, 90A25, 90A58

Key-words: Voronoi tessellation, Poisson process, Palm distribution, point process, communication network, interconnection cost.

[*] Postal address: INRIA-Ecole Normale Supérieure, Département de Mathématiques et d'Informatique, LIENS, 45 Rue d'Ulm, 75230 Paris, Cedex 05, France.
E-mail: Francois.Baccelli@ens.fr
[†] Postal address: CNET, 38 -40 Av. du General Leclerc, 92131 Issy Les Moulineaux, France.
E-mail: catherine.gloaguen@cnet.francetelecom.fr
[‡] Postal address: Statistics and Modelling Science dept., University of Strathclyde, Livingstone tower, 26 Richmond str., Glasgow G1 1XH, United Kingdom.
E-mail: sergei@stams.strath.ac.uk

Superposition de Pavages de Voronoï dans le Plan

Résumé : Nous étudions le pavage obtenu par intersection de deux pavages de Poisson-Voronoï du plan, dans le but d'obtenir des expressions en moyenne pour ses principales caractéristiques géometriques. Pour ce pavage intersection, nous distinguons six types de cellules suivant qu'elles contiennent ou non les noyaux des deux pavages de départ. L'intensité et la surface moyenne de chaque type de cellule sont calculées, soit de manière explicite, soit au moyen de développements asymptotiques. Ce modèle peut être utilisé pour représenter les zones locales de deux opérateurs de télécommunications en compétition sur le même territoire. Les coûts d'interconnexion entre les abonnés dépendent alors du type de cellule où ils se trouvent, les cellules étant précisément définies comme celles du pavage intersection associé à ces deux systèmes de zones locales.

Mots-clés : pavage de Voronoï, processus de Poisson, distribution de Palm, processus ponctuel, réseau de communications, inter-connexion

1 Introduction

1.1 Motivation

Point processes and stochastic geometry are used in a variety of research domains and have recently been applied to communication networks. The main idea consists in considering the spatial configuration of the network objects (subscribers, stations, links) as realizations of stochastic point or fiber processes, thus allowing one to take into account the irregularity of the actual spatial structure of the network. Then, quantities of interest such as cost functions or total length of connections, are expressed as functionals of these point processes, which allows for the solution of performance evaluation and optimization problems via a study of certain mathematical expectations. In its simplest form, a single hierarchical level telephone network consists of subscribers and switches, each of which serves the subscribers located in a certain area or cell. If the subscribers are served by and linked to their closest station, the cell system creates a random Voronoi tessellation of the plane, where the cell associated with a given switch represents the local zone of this switch. Detailed study of different models of that kind and discussions on assumptions and applicability of this approach can be found in [2], [1] and [4].

In the present paper, we use such a geometric model to represent the interconnection of subscribers of two competing telecommunication operators N_1 and N_2. In the basic model, the operators act independently and each of them possesses only one level of switches. Each set of switches defines an independent Voronoi tessellation, say T_1 for N_1 and T_2 for N_2, and thus a compound tessellation T, the cells of which are intersections of T_1 and T_2 cells. T cells are of different types depending on whether they contain switches of N_1 and N_2 or not. There are then at least six types of cells which are exemplified in Figures 1–3.

We assume below that for each operator, the cost incurred and charged for a call of a given subscriber depends on whether the communication remains within the cell of this operator (local call) or not (non-local call). Under this assumption, a communication between two subscribers, S_1 of N_1 and S_2 of N_2 belonging to the same cell T, induces different interconnection costs depending on the type of cell T. For instance, if the cell contains a switch of both N_1 and of N_2 (as for the cells of Figure 2 bottom), then the communication will be local for both operators and both subscribers. However if this cell contains a switch of N_1 and no switch of N_2, (as for the cells of Figure 3 top), then this communication will be non-local for S_1 and N_1 because the connection to S_2 goes via the switch of N_2 which is then outside the local zone of S_1.

Thus the analysis of the superposition of two Voronoi tessellations and in particular the computation of the mean area and of the intensity of each type of cell, gives a way to address predictively certain cost problems which arise in such a competitive situation.

1.2 Mathematical model

Let $\{x_i\}$ be an at most countable family of points in the plane $\mathbb{R}^2$. With each point x_i, one can associate a set $\mathcal{C}_{x_i}$ known as the *Voronoi cell* consisting of those points of $\mathbb{R}^d$ which are closer to x_i than to any other point $x_j,\ j \neq i$. The point x_i is called the *nucleus* of the cell $\mathcal{C}_{x_i}$. Since this set is the intersection of the half-planes $\{x:\ |x - x_i| \leq |x - x_j|\}$, $\mathcal{C}_{x_i}$ is a convex polygon. The collection of all these cells forms a *Voronoi tessellation* of the plane, meaning that every point of $\mathbb{R}^2$ (excluding a set of Lebesgue measure 0) belongs to a unique cell.

The main object of this study is the compound tessellation of the plane generated by the superposition of two Voronoi tessellations. Namely, let $N_1,\ N_2$ be two stationary point processes in $\mathbb{R}^2$ and let T_1 and T_2 denote the Voronoi tessellations generated by the points of N_1 and N_2, respectively. Then the superposition of these tessellations defines a new *compound tessellation* T. The set of boundaries of its cells is the union of the boundaries of T_1 and T_2. Since the set of points given by $N_1,\ N_2$ is random, then the tessellation T is also random in the sense that its boundary is a random closed set (cf. [5]).

Our aim is to characterize the distribution of the geometrical characteristics of "random representatives" of the cells of T. We show below that there are many ways of defining such a random representative:

- The first way is to take the cell $\dot{\mathcal{C}}$ which contains the origin 0. We will call it the *0-cell* in the sequel. It should be noted here that under stationary distribution assumptions for $N_1,\ N_2$, this cell is somewhat "larger" than other cells of T, since the origin is covered with bigger probability by cells of larger area. This is a spatial analogue of the well-known waiting time paradox for temporal point processes (see, e. g. [5, §6.2] or [8]).

- Although each Voronoi cell $\mathcal{C}^i$ constructed with respect to the points of the process N_i contains exactly one nucleus, this property is no longer true for the cells of T, which are defined as the intersection of two cells $\mathcal{C}^1_{x_i}$ and $\mathcal{C}^2_{y_j}$. In order to study the characteristics of cells of T which contain a nucleus, say of N_1 (necessarily unique), one may study the distribution of geometrical characteristics of the cell of T under the condition that there is a point of N_1 at the origin. For the tessellations we study this is possible since there is a one-to-one correspondence between these cells and the points of N_1. The interpretation of this distribution conditioned on a null-probability event is solved by considering the Palm distribution with respect to N_1.

- There are also cells of T which contain neither N_1 nor N_2 nuclei, so that the above view points are not sufficient. In order to study such cells, we will supply each cell of T with a unique reference point called its *centroid* and we will study the characteristics of the cell $\mathcal{C} = \mathcal{C}^1_{x_i} \cap \mathcal{C}^2_{y_j}$ under certain conditions such as:

  1. its centroid lies at the origin. This distribution would correspond to the distribution of a *typical cell* of T "chosen at random" among all the cells of T.

2. its centroid lies at the origin, and
   - the nuclei x_i and y_j are both in $\mathcal{C}$;
   - none of the nuclei x_i and y_j are in $\mathcal{C}$;
   - the nucleus y_j is not in $\mathcal{C}$, whereas x_i is in $\mathcal{C}$.

   This would correspond to the distribution of a typical cell of T which contains nuclei of both types, no nucleus, or only a nucleus of type N_1. This or the symmetrical case can be seen as refinements of what was considered above (see Figures 1–3).

Again, a rigorous interpretation of this conditioning is given by the Palm distributions with respect to both processes $N_1,\ N_2$ described later.

2 Notation and definitions.

2.1 Probability space, Palm probabilities

Throughout the paper we use the following notation:

$\mathcal{B}$: the Borel σ-algebra of subsets of the Euclidean space $\mathbb{R}^d$;

$|B|$: the Lebesgue measure of a Borel set $B \in \mathcal{B}$.

$\mathcal{N}$: the set of σ-finite counting measures on $\mathcal{B}$.

$\mathfrak{N}$: the σ-algebra of subsets of $\mathcal{N}$ generated by the system $\{\{\eta \in \mathcal{N}:\ \eta(B) = k\},\ B \in \mathcal{B},\ k \in \mathbb{N}\}$.

$(\Omega, \mathcal{F}, \mathbf{P})$: an abstract probability space.

$N_1,\ N_2$: random point processes, i.e. measurable mappings from $(\Omega, \mathcal{F}, \mathbf{P})$ to $[\mathcal{N}, \mathfrak{N}]$. Each realization $N_i(\omega)$ is an at most countable sum $\sum_i \delta_{x_i(\omega)}$ of Dirac measures, where $\delta_x(B) = \mathbb{I}_B(x)$. We assume that the processes N_i are *simple*, i.e. with probability 1, all $x_i(\omega)$ are distinct. In this case there is a bijection between $N_i(\omega)$ and the set of its support points supp $N_i(\omega) = \{x_i(\omega)\}_i$.

$\Pi_1,\ \Pi_2$: independent homogeneous Poisson point processes with intensities ν_i $(i = 1,\ 2)$, i.e. the point processes for which $\Pi_i(B)$ has a Poisson distribution with parameter $\nu_i|B|$, for any $B \in \mathcal{B}$ with $|B| < \infty$, and such that the variables $\Pi_i(B_1),\ \Pi_i(B_2)$ are independent for all $B_1 \cap B_2 = \emptyset$.

$\mathbf{P}_i$: the Palm distribution with respect to the process N_i, see (1).

We will intensively use Palm calculus for stationary point processes. Let us recall the main definitions.

The addition operation in $\mathbb{R}^d$ gives rise to measurable *flows* in $[\mathbb{R}^d, \mathcal{B}]$ and in $[\mathcal{N}, \mathfrak{B}]$, defined as $\theta_x B = B + x = \{y + x :\ y \in B\}$ for $B \in \mathcal{B}$ and $(\theta_x \eta)(B) \stackrel{\text{def}}{=} \eta(\theta_x B)$ for $\eta \in \mathcal{N}$

and all $B \in \mathcal{B}$. In particular, if $N = \sum_i \delta_{x_i}$ then $\theta_x N = \sum_i \delta_{x_i - x}$. The point process N is *stationary* with respect to the flow $\theta_\bullet$ if the distributions of N and $\theta_x N$ coincide for all $x \in X$. If N is a stationary process, for any Borel B one has $\mathbf{E}\, N(B) = \lambda_N |B|$, for some positive constant λ_N called the *intensity* of N.

When dealing with several point processes, it is sometimes convenient to introduce a shift φ_x, $x \in X$ on the probability space $(\Omega, \mathcal{F}, \mathbf{P})$, which is assumed to preserve $\mathbf{P}$, and to assume that this shift is *compatible* with the translations $\theta_\bullet$ in $\mathbb{R}^d$, namely that

$$N_i(\varphi_x \omega) = \theta_x N_i(\omega),$$

for all i, x and ω. The *Palm probability* of an event $\Xi \in \mathcal{F}$ with respect to N_i is then defined by

$$\mathbf{P}_i(\Xi) = \frac{1}{\lambda_{N_i} |B|}\, \mathbf{E} \int_B \mathbb{1}_\Xi(\varphi_x \omega)\, N_i(dx)\,, \tag{1}$$

where λ_{N_i} is the intensity of the process N_i; it can be shown to be independent of the choice of $B \in \mathcal{B}$. The expectation with respect to $\mathbf{P}_i$ is denoted by $\mathbf{E}_i$. The intuitive meaning is that of the conditional distribution "given there is a point of the process N_i at the origin 0". By the standard monotone class argument, the following identities can be directly derived from this definition :

$$\mathbf{E}_i\, f(\omega) = \frac{1}{\lambda_{N_i} |B|}\, \mathbf{E} \int_B f(\varphi_x \omega)\, N_i(dx)\,, \tag{2}$$

$$\mathbf{E} \int F(x, \omega)\, N_i(dx) = \lambda_{N_i} \int \mathbf{E}_i\, F(x, \varphi_{-x} \omega)\, dx \tag{3}$$

for any measurable functions $f:\ \Omega \to \mathbb{R}_+$ and $F:\ \mathbb{R}^d \times \Omega \mapsto \mathbb{R}_+$. The last formula is known as the *refined Campbell formula* for stationary marked processes (cf. [12, Formula (4.4.11)]).

Formula (2) provides another useful interpretation of $\mathbf{E}_i$ as an *ergodic mean*. Assume that $f(\omega)$ is some characteristic of the configuration when the origin is a point of the support of N_i. When the set B becomes "large", then by the Law of Large Numbers, the RHS of (2) is equivalent to

$$\frac{1}{N_i(B)} \sum_{x_i \in N_i \cap B} f(\varphi_{x_i} \omega),$$

that is the mean value of f "seen from" the points of N_i located in B (cf. [3, Prop.12.4.I]). This allows one to interpret $\mathbf{E}_i\, f$ as the value of f at a *typical* point of the process N_i.

The particular case where $N_i = \Pi_i$, $i = 1,\ 2$, a homogeneous Poisson processes in the plane, and where the point processes Π_1, Π_2 are independent, which is considered in the paper, can, of course, be embedded within the above framework. For a Poisson process Π_i, its Palm distribution $\mathbf{P}_i$ coincides with the $\mathbf{P}$-distribution of the processes $\Pi + \delta_0$, i.e. the process with an additional point at the origin 0. This is known as Slivnyak's theorem and is, in fact, another characterization of Poisson processes (see, e. g., [12, p.121]).

Let now $g : \Omega \mapsto \mathbb{R}_+$ be a measurable function. The following identity expresses the relationship between the Palm and the original distribution of a marked stationary point process (cf. [3, Formula (12.3.13)]) :

$$\mathbf{E}\, g(\omega) = \lambda_{N_i}\, \mathbf{E}_i \int_{\mathcal{C}_0^i} g(\varphi_x \omega)\, dx\,. \tag{4}$$

The set $\mathcal{C}_0^i$ above is the Voronoi cell *with nucleus* 0 constructed with respect to the point set N_i (note that, under the Palm distribution $\mathbf{P}_i$, there is a.s. a point of N_i at the origin 0 and therefore $\mathcal{C}_0^i$ coincides with the 0-cell $\dot{\mathcal{C}}^i$).

The following exchange formula relates two Palm distributions and can be obtained by taking $a(\omega, t)$ equal to the indicator of the event "t is the point of the process $N_1(\omega)$ which is the closest to the origin", in the remark following the proof of Proposition 1 in Neveu [10, p.201]:

$$\lambda_{N_1}\, \mathbf{E}_1\, f(\omega) = \lambda_{N_2}\, \mathbf{E}_2 \int_{\mathcal{C}_0^2} f(\varphi_x \omega)\, N_1(dx), \tag{5}$$

for any measurable $f :\ \Omega \mapsto \mathbb{R}_+$.

2.2 The point process of centroids

Centroids Each compound cell $\mathcal{C}$ is the non-empty intersection of two cells $\mathcal{C}^1_{x_i}$ and $\mathcal{C}^2_{y_j}$, where $\mathcal{C}^i_u$ denotes the Voronoi cell with nucleus $u \in N_i$ constructed with respect to the points of N_i. We define the *centroid* $z(\mathcal{C})$ of $\mathcal{C}$ as its center of gravity. So, a compound cell always contains its centroid.

By construction, there is one-to-one correspondence between the compound cells and their centroids, which is in addition compatible with the flow $\varphi_{\bullet}$:

$$z(\mathcal{C}(\varphi_x \omega)) = \theta_x\, z(\mathcal{C}(\omega))\,.$$

This property implies that the point process Z of the centroids is also stationary. This enables one to define the Palm probability with respect to Z as follows:

$$\mathbf{P}_Z(\Xi) = \frac{1}{\lambda_Z |B|}\, \mathbf{E} \int_B \mathbb{1}_{\Xi}(\varphi_x \omega)\, Z(dx)\,, \tag{6}$$

where $\Xi \in \mathcal{F}$ and $\lambda_Z = \mathbf{E}\, Z([0,1]^2)$ is the intensity of centroids (of the compound tessellation cells).

The probability $\mathbf{P}_Z$ can be interpreted as the law of a configuration with a centroid of the compound tessellation at the origin. Therefore under $\mathbf{P}_Z$ the cell whose centroid lies at the origin is exactly the 0-cell $\dot{\mathcal{C}} = \dot{\mathcal{C}}^1 \cap \dot{\mathcal{C}}^2$.

Other point processes As mentioned in the introduction, several subprocesses of the point process Z will also be of use:

$Z^{[1,2]}$: the subprocess of Z which only keeps the centroids $z(\mathcal{C}) = z(\mathcal{C}^1_{x_i} \cap \mathcal{C}^2_{y_j})$ such that $x_i \in \mathcal{C}$ and $y_j \in \mathcal{C}$.

$Z^{[\overline{1},\overline{2}]}$: the subprocess of Z which only keeps the centroids of cells $\mathcal{C}$ such that $x_i \notin \mathcal{C}$ and $y_j \notin \mathcal{C}$.

$Z^{[1,\overline{2}]}$: the subprocess of Z which only keeps the centroids such that $x_i \in \mathcal{C}$ and $y_j \notin \mathcal{C}$ (and the symmetrical case).

$Z^{[1]}$: the subprocess of Z which only keeps the centroids such that $x_i \in \mathcal{C}$ (and the symmetrical cases).

Each of these subprocesses is compatible with the flow $\varphi_\bullet$, so that to each of them, one can associate a Palm probability. The following notation will be used: $\mathbf{P}_Z^{[\overline{1},\overline{2}]}$, $\mathbf{P}_Z^{[1,2]}$, $\mathbf{P}_Z^{[1,\overline{2}]}$, $\mathbf{P}_Z^{[1]}$ etc., with an obvious signification.

One can also define Palm probabilities with respect to other point processes related to the tessellation T, such as the process of cell vertices, edge middle-points, etc.

Characteristics We will use the following standard notations for the pathwise characteristics of the tessellation T:

$n_{20}(\dot{\mathcal{C}})$: the number of vertices of $\dot{\mathcal{C}}$,

$l_2(\dot{\mathcal{C}})$: the perimeter of $\dot{\mathcal{C}}$,

$|\dot{\mathcal{C}}|$: the area of $\dot{\mathcal{C}}$,

Thus $\mathbf{E}_Z\, n_{20}(\dot{\mathcal{C}})$, $\mathbf{E}_Z\, l_2(\dot{\mathcal{C}})$, $\mathbf{E}_Z\, |\dot{\mathcal{C}}|$ can be interpreted as the mean characteristics of a "typical cell" of T. As it was already mentioned, the distribution of $\dot{\mathcal{C}}$ under $\mathbf{P}$ is *different* from the one of a typical cell. The above expectations can of course also be considered under the Palm probabilities of any of the other subprocesses.

Finally, the following notations will be used for the intensities and mean values related to T:

$\lambda_0,\ \lambda_1,\ \lambda_2$: the intensity of the vertices, centers of edges and of the compound cell centroids, respectively (note that $\lambda_2 = \lambda_Z$).

$\bar{n}_{02}$: the mean number of cells meeting in a typical vertex.

$\bar{l}_0$: the mean total length of edges emanating from a typical vertex.

$\bar{l}_1$: the mean length of a typical edge.

$L_A,\ L_A^{(i)}$: the mean length of edges of T (resp., $T_i,\ i = 1,2$) per unit area.

3 Ergodic characteristics of the compound tessellation

This section is mainly based on the *mean characteristics relationships* for planar tessellations established in [6] (see also [12, §10.3]), which give expressions for all quantities λ_1, λ_2, $\bar{l}_0$, $\bar{l}_1$, $\mathbf{E}_Z\, l_2(\dot{\mathcal{C}})$, $\mathbf{E}_Z\, |\dot{\mathcal{C}}|$, and $\mathbf{E}_Z\, n_{20}(\dot{\mathcal{C}})$ from the three basic variables λ_0, $\mathbf{E}_Z\, n_{02}$ and L_A only. We also use exact expressions for mean values of the Voronoi tessellation geometric characteristics that can be found, e. g., in [9]. Although formulae (9), (19) and (20) have already been obtained in [11] we give their proofs for the sake of a uniformity of the presentation.

Throughout the section, T_1 and T_2 are the Voronoi tessellations generated by two *independent Poisson* processes Π_1 and Π_2, with respective intensities ν_1 and ν_2.

3.1 Intensities

We first focus on $\lambda_0 = \lambda_0(T)$, the intensity of the point process of vertices in the tessellation T, described in Section 2 above.

To find λ_0, we first compute the intensity γ of the points which are intersections of edges of the tessellations T_1 and T_2. The general formula was obtained in [7, Th.3.1]. Since Π_i is Poisson, the mean total length of edges of T_i in a unit square is

$$L_A^{(i)} = 2\sqrt{\nu_i}.$$

Therefore from Mecke's Theorem 3.1,

$$\gamma = \frac{2}{\pi} L_A^{(1)} L_A^{(2)} = \frac{8}{\pi}\sqrt{\nu_1 \nu_2}\,.$$

Since the vertices of the compound cells are either the vertices of T_1 and T_2 or these intersection points, then

$$\lambda_0(T) = \lambda_0(T_1) + \lambda_0(T_2) + \frac{8}{\pi}\sqrt{\nu_1\nu_2} = 2(\nu_1 + \nu_2) + \frac{8}{\pi}\sqrt{\nu_1\nu_2}\,. \tag{7}$$

In the vertices of each Voronoi tessellation, exactly 3 cells meet, while in the above intersection points, this number is 4. Thus, taking into account the densities of both types of vertices we get

$$\bar{n}_{02} = 6\frac{\nu_1 + \nu_2}{\lambda_0} + 32\frac{\sqrt{\nu_1\nu_2}}{\pi\lambda_0}\,. \tag{8}$$

Using the mean characteristics relationships, we get the following values for the centroid intensity and for the edge center intensity:

$$\lambda_2 = \lambda_0(\bar{n}_{02}/2 - 1) = \nu_1 + \nu_2 + \frac{8}{\pi}\sqrt{\nu_1\nu_2}\,; \tag{9}$$

$$\lambda_1 = \lambda_0 + \lambda_2 = 3(\nu_1 + \nu_2) + \frac{16}{\pi}\sqrt{\nu_1\nu_2}\,; \tag{10}$$

We now concentrate on $\lambda_2^{[\overline{1},\overline{2}]}$, $\lambda_2^{[\overline{1},2]}$, $\lambda_2^{[1,\overline{2}]}$ and $\lambda_2^{[1,2]}$, which respectively denote the intensities of the stationary point processes $Z^{[\overline{1},\overline{2}]}$, $Z^{[\overline{1},2]}$, $Z^{[1,\overline{2}]}$ and $Z^{[1,2]}$.

Let $D_y(x)$ denote the open disc centered in $x \in \mathbb{R}^2$ and such that $y \in \mathbb{R}^2$ belongs to its boundary. Each cell $\mathcal{C}$ with a centroid belonging to $Z^{[1,2]}$ is the intersection of two cells $\mathcal{C}_x^1$ and $\mathcal{C}_y^2$ such that $x \in \mathcal{C}_y^2$ and $y \in \mathcal{C}_x^1$. Therefore the points of $Z^{[1,2]}$ are in bijection with the point $x \in \Pi_1$ with the following property: if $y = y(x)$ is the closest point of Π_2, namely the a.s. unique point of Π_2 such that

$$\Pi_2\big(D_y(x)\big) = 0\,,$$

then

$$\Pi_1\big(D_x(y)\big) = 0\,.$$

The probability of the last event is

$$\mathbf{P}_1\big\{y(0) \in \dot{\mathcal{C}}^1\big\} = \nu_2 \int e^{-\nu_1\pi\|y\|^2} e^{-\nu_2\pi\|y\|^2}\,dy = 2\pi\nu_2 \int_0^\infty e^{-(\nu_1+\nu_2)\pi r^2}\,rdr = \frac{\nu_2}{\nu_1+\nu_2}\,.$$

Therefore, the intensity of the points $x_i \in \Pi_1$ such that the above property holds (and thus the intensity of $Z^{[1,2]}$) is equal to

$$\lambda_2^{[1,2]} = \frac{\nu_1\nu_2}{\nu_1+\nu_2}\,. \tag{11}$$

Consequently,

$$\lambda_2^{[1,\overline{2}]} = \lambda_2^{[1]} - \lambda_2^{[1,2]} = \nu_1 - \lambda_2^{[1,2]} = \frac{\nu_1^2}{\nu_1+\nu_2}\,. \tag{12}$$

Similarly,

$$\lambda_2^{[\overline{1},2]} = \frac{\nu_2^2}{\nu_1+\nu_2}\,, \tag{13}$$

and, finally,

$$\lambda_2^{[\overline{1},\overline{2}]} = \lambda_2 - \big(\lambda_2^{[1,2]} + \lambda_2^{[1,\overline{2}]} + \lambda_2^{[\overline{1},2]}\big) = \frac{\nu_1\nu_2}{\nu_1+\nu_2} + \frac{8}{\pi}\sqrt{\nu_1\nu_2}\,. \tag{14}$$

3.2 Mean geometric characteristics of a typical cell

Evidently, for the mean length of edges of T per unit area one has

$$L_A = L_A^{(1)} + L_A^{(2)}\,. \tag{15}$$

This, together with expressions (7-8) for λ_0 and for $\bar{n}_{02}$ above, allows one to express other mean ergodic characteristics of the compound tessellation T. The mean length of a typical edge:

$$\bar{l}_1 = \frac{L_A}{\lambda_1} = \frac{2\big(\sqrt{\nu_1} + \sqrt{\nu_2}\big)}{3(\nu_1 + \nu_2) + \frac{16}{\pi}\sqrt{\nu_1 \nu_2}}\,; \tag{16}$$

the mean total length of the edges emanating from a typical vertex:

$$\bar{l}_0 = \frac{2L_A}{\lambda_0} = \frac{2\big(\sqrt{\nu_1} + \sqrt{\nu_2}\big)}{\nu_1 + \nu_2 + \frac{4}{\pi}\sqrt{\nu_1 \nu_2}}\,; \tag{17}$$

the mean area of a typical cell:

$$\mathbf{E}_Z\,|\dot{\mathcal{C}}| = \frac{1}{\lambda_2} = \Big[\nu_1 + \nu_2 + \frac{8}{\pi}\sqrt{\nu_1 \nu_2}\Big]^{-1}\,; \tag{18}$$

the mean perimeter:

$$\mathbf{E}_Z\,l_2(\dot{\mathcal{C}}) = \frac{2L_A}{\lambda_2} = \frac{4\big(\sqrt{\nu_1} + \sqrt{\nu_2}\big)}{\nu_1 + \nu_2 + \frac{8}{\pi}\sqrt{\nu_1 \nu_2}}\,. \tag{19}$$

Finally, the typical cell contains on average

$$\mathbf{E}_Z\,n_{20}(\dot{\mathcal{C}}) = 2 + \frac{2\lambda_0}{\lambda_2} = \frac{6(\nu_1 + \nu_2) + \frac{32}{\pi}\sqrt{\nu_1 \nu_2}}{\nu_1 + \nu_2 + \frac{8}{\pi}\sqrt{\nu_1 \nu_2}} \tag{20}$$

vertices (and edges). In particular, the minimal value of $\mathbf{E}_Z\,n_{20}(\dot{\mathcal{C}})$ is $\frac{6\pi+16}{\pi+4} \approx 4.8798$, attained when $\nu_1 = \nu_2$.

4 Integral formulae for the mean area of the 0-cell

In this section we are interested in the mean area of the 0-cell $\dot{\mathcal{C}}$ of T under various Palm probabilities.

4.1 Mean area under $\mathbf{P}_i$

Let us take $i = 1$. Using the notation introduced above, and polar coordinates, we get the following representation:

$$\begin{aligned}
\mathbf{E}_1 |\dot{\mathcal{C}}| &= \mathbf{E}_1 \left| \dot{\mathcal{C}}^1 \cap \dot{\mathcal{C}}^2 \right| \\
&= \int_0^{2\pi} \int_0^{\infty} \mathbf{E}_1 \left\{ \mathbb{I}_{(r,\theta)\in\dot{\mathcal{C}}^1} \, \mathbb{I}_{(r,\theta)\in\dot{\mathcal{C}}^2} \right\} r dr d\theta \\
&= \int_0^{2\pi} \int_0^{\infty} \mathbf{P}_1 \left\{ (r,\theta) \in \dot{\mathcal{C}}^1 \right\} \mathbf{P} \left\{ (r,\theta) \in \dot{\mathcal{C}}^2 \right\} r dr d\theta \\
&= 2\pi \int_0^{\infty} \mathbf{P}_1 \left\{ (r,0) \in \dot{\mathcal{C}}^1 \right\} \mathbf{P} \left\{ (r,0) \in \dot{\mathcal{C}}^2 \right\} r dr,
\end{aligned}$$

where we used the independence between Π_1 and Π_2 to obtain the third relation and isotropy to derive the last one.

Since Π_1 is Poisson of intensity ν_1, it follows from Slivnyak's theorem that

$$\mathbf{P}_1 \left\{ (r,0) \in \dot{\mathcal{C}}^1 \right\} = e^{-\nu_1 \pi r^2}. \tag{21}$$

Now Campbell's refined formula yields

$$\begin{aligned}
\mathbf{P} \left\{ (r,0) \in \dot{\mathcal{C}}^2 \right\} &= \mathbf{E} \, \mathbb{I}_{(r,0)\in\dot{\mathcal{C}}^2} \\
&= \mathbf{E} \int \mathbb{I}_{(0,0)\in C_x^2} \, \mathbb{I}_{(r,0)\in C_x^2} \, \Pi_2(dx) \\
&= \int \mathbf{P}_2 \left\{ \mathbb{I}_{(0,0)\in C_x^2(\varphi_{-x}\omega)} \, \mathbb{I}_{(r,0)\in C_x^2(\varphi_{-x}\omega)} \right\} \nu_2 dx \\
&= \int \mathbf{P} \left\{ N_2(D_x((0,0)) \cup D_x((r,0)) = 0 \right\} \nu_2 dx,
\end{aligned}$$

where we used Slivnyak's Theorem to obtain the last relation. Let $(\|x\|, \theta)$ be the polar coordinate representation of x, and for $r > 0$, let $\|x\| = \alpha r$. Representing now x in the coordinates (α, θ), we obtain that

$$\mathbf{P} \left\{ (r,0) \in \dot{\mathcal{C}}^2 \right\} = 2\nu_2 r^2 \int_0^{\pi} \int_0^{\infty} e^{-\nu_2 r^2 A(1,\alpha,\theta)} \, \alpha d\alpha d\theta \,, \tag{22}$$

where $A(r,\alpha,\theta)$ denotes the area of the union of the two discs $D_{(r\alpha,\theta)}\big((0,0)\big)$ and $D_{(r\alpha,\theta)}\big((r,0)\big)$ (see Figure 4).

It follows from classical geometrical arguments that $A(1,\alpha,\theta) \stackrel{\text{def}}{=} A(\alpha,\theta)$ with

$$A(\alpha,\theta) = \alpha\sin\theta + \alpha^2(\pi-\theta) + \left(\alpha^2+1-2\alpha\cos\theta\right)\left(\pi - \arccos\frac{1-\alpha\cos\theta}{\sqrt{\alpha^2+1-2\alpha\cos\theta}}\right). \tag{23}$$

We obtain from (21) and (22) that

$$\mathbf{E}_1\,|\dot{\mathcal{C}}| = 2\pi\int_0^\infty re^{-\nu_1\pi r^2}Q(\nu_2,r)dr\,, \tag{24}$$

with

$$Q(\nu,r) = 2\nu r^2\int_0^\pi\int_0^\infty e^{-\nu r^2 A(\alpha,\theta)}\alpha d\alpha d\theta, \tag{25}$$

and with $A(\alpha,\theta)$ defined by (23). Let $u=\sqrt{\nu}r$. Then $Q(\nu,r) = 2P(u^2)$ with

$$P(v) = v\int_0^\pi\int_0^\infty e^{-A(\alpha,\theta)v}\alpha d\alpha d\theta,$$

so that

$$\begin{aligned}
\mathbf{E}_1\,|\dot{\mathcal{C}}| &= \frac{4\pi}{\nu_2}\int_0^\infty ue^{-\pi\frac{\nu_1}{\nu_2}u^2}P(u^2)du \\
&= \frac{2\pi}{\nu_2}\int_0^\infty e^{-\pi\frac{\nu_1}{\nu_2}v}P(v)dv \\
&= \frac{2\pi}{\nu_2}\int_0^\pi\int_0^\infty\left[\int_0^\infty e^{-\pi\frac{\nu_1}{\nu_2}v}e^{-A(\alpha,\theta)v}\,vdv\right]\alpha d\alpha d\theta.
\end{aligned}$$

Finally, we get the following representation, to be used later:

$$\mathbf{E}_1\,|\dot{\mathcal{C}}| = \frac{2\pi}{\nu_2}\int_0^\pi\int_0^\infty\frac{\alpha}{\left(\pi\frac{\nu_1}{\nu_2}+A(\alpha,\theta)\right)^2}\,d\alpha d\theta. \tag{26}$$

4.2 Mean area under P

By the same arguments,

$$\begin{aligned}
\mathbf{E}\,|\dot{\mathcal{C}}| &= \mathbf{E}\,\big|\,\dot{\mathcal{C}}^1\cap\dot{\mathcal{C}}^2\big| \\
&= 2\pi\int_0^\infty Q(\nu_1,r)Q(\nu_2,r)\,r\,dr \\
&= 2\pi\int_{[0,\pi]^2}\int_{[0,\infty)^2} 4\nu_1\nu_2\alpha_1\alpha_2 \\
&\qquad\times\int_0^\infty r^5 e^{-r^2(\nu_1 A(\alpha_1,\theta_1)+\nu_2 A(\alpha_2,\theta_2))}dr\ d\alpha_1 d\alpha_2 d\theta_1 d\theta_2 \\
&= 4\pi\nu_1\nu_2\int_{[0,\pi]^2}\int_{[0,\infty)^2}\int_0^\infty v^2 e^{-v(\nu_1 A(\alpha_1,\theta_1)+\nu_2 A(\alpha_2,\theta_2))}dv d\alpha_1 d\alpha_2 d\theta_1 d\theta_2\,,
\end{aligned}$$

so that

$$\mathbf{E}\,|\dot{\mathcal{C}}| = 8\pi\nu_1\nu_2\int_{[0,\pi]^2}\int_{[0,\infty)^2}\frac{\alpha_1\alpha_2}{\big(\nu_1 A(\alpha_1,\theta_1)+\nu_2 A(\alpha_2,\theta_2)\big)^3}d\alpha_1 d\alpha_2 d\theta_1 d\theta_2\,. \tag{27}$$

4.3 Mean area under $\mathbf{P}_Z^{[1,2]}$

Using the same bijection as in § 3.1 and the results obtained there, we get

$$\begin{aligned}
\mathbf{E}_Z^{[1,2]}\,|\dot{\mathcal{C}}| &= \mathbf{E}_1\left[|\mathcal{C}_0^1\cap\mathcal{C}_{y(0)}^2|\ \big|\ y(0)\in\mathcal{C}_0^1\right] \\
&= \big(\mathbf{P}_1\{y(0)\in\mathcal{C}_0^1\}\big)^{-1}\,\mathbf{E}_1\left[|\mathcal{C}_0^1\cap\mathcal{C}_{y(0)}^2|\,\mathbb{1}_{y(0)\in\mathcal{C}_0^1}\right] \\
&= \frac{\nu_1+\nu_2}{\nu_2}\,\mathbf{E}_1\left[|\mathcal{C}_0^1\cap\mathcal{C}_{y(0)}^2|\ \ \mathbb{1}_{y(0)\in\mathcal{C}_0^1}\right].
\end{aligned}$$

We have

$$\begin{aligned}
\mathbf{E}_1\left[|\mathcal{C}_0^1\cap\mathcal{C}_{y(0)}^2|\ \ \mathbb{1}_{y(0)\in\mathcal{C}_0^1}\right] &= \nu_2\int\mathbf{E}_1\left[|\mathcal{C}_0^1\cap\mathcal{C}_y^2|\ \ \mathbb{1}_{y\in\mathcal{C}_0^1}\ \mathbb{1}_{\Pi_2(D_y(0))=0}\right]dy \\
&= \nu_2\iint\mathbf{E}_1\left[\mathbb{1}_{x\in\mathcal{C}_0^1}\ \mathbb{1}_{y\in\mathcal{C}_0^1}\ \mathbb{1}_{x\in\mathcal{C}_y^2}\ \mathbb{1}_{\Pi_2(D_y(0))=0}\right]dxdy \\
&= \nu_2\iint\exp\{-\nu_1|D_0(x)\cup D_0(y)|-\nu_2|D_y(0)\cup D_y(x)|\}\,dxdy\,.
\end{aligned}$$

Introducing the coordinate change

$$\begin{cases} x_1 &= r\cos\theta \\ x_2 &= r\sin\theta \\ y_1 &= x_1 - r\alpha\cos(\varphi+\theta) \\ y_2 &= x_2 - r\alpha\sin(\varphi+\theta) \end{cases}$$
$$0 < r, \alpha < \infty\,,\ 0 \le \theta < 2\pi\,,\ -\pi \le \varphi < \pi\,;$$

(see Figure 5) we obtain that

$$\mathbf{E}_Z^{[1,2]}\,|\dot{\mathcal{C}}| = 2(\nu_1+\nu_2)\int_0^{2\pi} d\theta \int_0^{\infty} r^3 dr \int_0^{\pi} d\varphi \int_0^{\infty} \alpha d\alpha \exp\{-\nu_1 A(\alpha r, \alpha^{-1}, \varphi) - \nu_2 A(r,\alpha,\varphi)\}\,,$$

where $A(r,\alpha,\varphi)$ is the function defined in § 4.1. Continuing as above, we finally get

$$\mathbf{E}_Z^{[1,2]}\,|\dot{\mathcal{C}}| = 2\pi(\nu_1+\nu_2)\int_0^{\pi}\int_0^{\infty} \frac{\alpha d\alpha d\varphi}{\big(\nu_1\alpha^2 A(\alpha^{-1},\varphi) + \nu_2 A(\alpha,\varphi)\big)^2} \tag{28}$$

4.4 Mean area under $\mathbf{P}_Z^{[1,\bar{2}]}$, $\mathbf{P}_Z^{[\bar{1},2]}$ and $\mathbf{P}_Z^{[\bar{1},\bar{2}]}$

Proceeding as in the previous section, we can write

$$\mathbf{E}_Z^{[1,\bar{2}]}\,|\dot{\mathcal{C}}| = \mathbf{E}_1\left[|\mathcal{C}_0^1 \cap \mathcal{C}_{y(0)}^2| \;\Big|\; y(0) \notin \mathcal{C}_0^1\right]\,.$$

But

$$\begin{aligned} \mathbf{E}_1\,|\dot{\mathcal{C}}| &= \mathbf{E}_1\left[|\mathcal{C}_0^1 \cap \mathcal{C}_{y(0)}^2| \;\Big|\; y(0) \in \mathcal{C}_0^1\right]\,\mathbf{P}_1\{y(0)\in\mathcal{C}_0^1\} \\ &\quad + \mathbf{E}_1\left[|\mathcal{C}_0^1 \cap \mathcal{C}_{y(0)}^2| \;\Big|\; y(0) \notin \mathcal{C}_0^1\right]\,\mathbf{P}_1\{y(0)\notin\mathcal{C}_0^1\} \\ &= \frac{\nu_2}{\nu_1+\nu_2}\,\mathbf{E}_Z^{[1,2]}\,|\dot{\mathcal{C}}| + \frac{\nu_1}{\nu_1+\nu_2}\,\mathbf{E}_Z^{[1,\bar{2}]}\,|\dot{\mathcal{C}}|\,. \end{aligned}$$

Therefore

$$\mathbf{E}_Z^{[1,\bar{2}]}\,|\dot{\mathcal{C}}| = \left(1+\frac{\nu_2}{\nu_1}\right)\mathbf{E}_1\,|\dot{\mathcal{C}}| - \frac{\nu_2}{\nu_1}\,\mathbf{E}_Z^{[1,2]}\,|\dot{\mathcal{C}}|\,, \tag{29}$$

and the final integral expression is obtained after substitution of formulae (26) and (28). Obviously, the expression for $\mathbf{E}_Z^{[\bar{1},2]}\,|\dot{\mathcal{C}}|$ is the same except that ν_1 and ν_2 are interchanged.

Finally,

$$1 = \lambda_2\,\mathbf{E}_Z\,|\dot{\mathcal{C}}| = \lambda_2^{[1,2]}\,\mathbf{E}_Z^{[1,2]}\,|\dot{\mathcal{C}}| + \lambda_2^{[\bar{1},2]}\,\mathbf{E}_Z^{[\bar{1},2]}\,|\dot{\mathcal{C}}| + \lambda_2^{[1,\bar{2}]}\,\mathbf{E}_Z^{[1,\bar{2}]}\,|\dot{\mathcal{C}}| + \lambda_2^{[\bar{1},\bar{2}]}\,\mathbf{E}_Z^{[\bar{1},\bar{2}]}\,|\dot{\mathcal{C}}|\,, \tag{30}$$

from where and from (9), (11)–(14), (28), (29) the expression for $\mathbf{E}_Z^{[\bar{1},\bar{2}]}\,|\dot{\mathcal{C}}|$ can be easily derived.

4.5 Example

Table 1 below gathers numerical results for all the mean values considered above. Let

$$x = \frac{\nu_1}{\nu_2}.$$

Four cases are considered: $x \downarrow 0$, with $\nu_1 \downarrow 0$ and $\nu_2 = 1$; $x = 0.6$, with $\nu_1 = 0.6$ and $\nu_2 = 1$; $x = 1$, with $\nu_1 = 1$ and $\nu_2 = 1$; $x = \infty$, with $\nu_1 = 1$ and $\nu_2 \downarrow 0$.

The first value given in each entry is the mean area under the Palm measure for the type of cell which is considered. The value in brackets is the proportion of the plane which is covered by this type of cells (product of the first entry and the intensity of the corresponding cells - see Figure 6). The variations of $\mathbf{E}_1 |\dot{\mathcal{C}}|$, $\mathbf{E}_2 |\dot{\mathcal{C}}|$, $\mathbf{E}_Z^{[1,2]} |\dot{\mathcal{C}}|$ seen as functions of x, are shown in Figure 8.

	$x \downarrow 0$		$x = 0.6$	$x = 1$	$x \uparrow \infty$	
$\mathbf{E}_Z |\dot{\mathcal{C}}|$	$1.00 - 2.5x$	[1.00]	0.28 [1.00]	0.22 [1.00]	$1 - 2.5/x$	[1.00]
$\mathbf{E} |\dot{\mathcal{C}}|$	$1.28 - 1.08\sqrt{x}$	[—]	0.60 [—]	0.48 [—]	$1.28 - 1.08/\sqrt{x}$	[—]
$\mathbf{E}_1 |\dot{\mathcal{C}}|$	$1.28 - 2.31x$	[0.00]	0.63 [0.38]	0.48 [0.48]	$1 - 2/(\pi\sqrt{x})$	[1.00]
$\mathbf{E}_2 |\dot{\mathcal{C}}|$	$1.00 - 2/\pi\sqrt{x}$	[1.00]	0.57 [0.57]	0.48 [0.48]	$1.28 - 2.31/x$	[0.00]
$\mathbf{E}_Z^{[1,2]} |\dot{\mathcal{C}}|$	$1.28 - 1.73x$	[0.00]	0.74 [0.28]	0.59 [0.30]	$1.28 - 1.73/x$	[0.00]
$\mathbf{E}_Z^{[\bar{1},2]} |\dot{\mathcal{C}}|$	$1.00 - 2/\pi\sqrt{x}$	[1.00]	0.47 [0.29]	0.36 [0.18]	$0.69 - 0.7/x$	[0.00]
$\mathbf{E}_Z^{[1,\bar{2}]} |\dot{\mathcal{C}}|$	$0.69 - 0.7x$	[0.00]	0.44 [0.10]	0.36 [0.18]	$1.00 - 2/(\pi\sqrt{x})$	[1.00]
$\mathbf{E}_Z^{[\bar{1},\bar{2}]} |\dot{\mathcal{C}}|$	$0.25 - 0.13\sqrt{x}$	[0.00]	0.14 [0.33]	0.11 [0.34]	$1.25 - 0.13/\sqrt{x}$	[0.00]

Table 1: The mean area of different types of cells.

5 Asymptotic expansions and numerical results for the area of the 0-cell

Numerical tools, e. g. the package Mathematica, can be used to evaluate the integral expressions obtained in the previous section for particular values of ν_1 and ν_2. Some of the results are gathered in the tables of § A. An alternative approach, that we consider in this section, is based on asymptotic expansions of the functions under the multiple integrals with subsequent explicit evaluation of the terms. It may be particularly useful when one needs to consider a variety of different values for the intensities, and can be easily programmed. The corresponding Microsoft Excel program can be obtained from *ftp://ftp.stams.strath.ac.uk/~/pub/sergei/Vcells.xls*. Since relation (30) holds it is sufficient to consider just three cases: $\mathbf{E}_1 |\dot{\mathcal{C}}|$, $\mathbf{E} |\dot{\mathcal{C}}|$ and $\mathbf{E}_Z^{[1,2]} |\dot{\mathcal{C}}|$ below.

5.1 Expectation of the area of $\dot{\mathcal{C}}$ with respect to $\mathbf{P}_1$

In Section 4.1 we have obtained an integral formula (26) for the mean area of the cell under distribution $\mathbf{P}_1$. Denoting $x = \nu_1/\nu_2$, expression (26) can be rewritten as

$$\mathbf{E}_1 |\dot{\mathcal{C}}| = \frac{2\pi}{\nu_2} f(x)\,,$$

where

$$f(x) = \iint\limits_D \frac{\alpha d\alpha d\theta}{(\pi x + A(\alpha,\theta))^2} \tag{31}$$

in the integration domain $D = [0,\infty) \times [0,\pi]$, where $A(\alpha,\theta)$ is given by (23). Such an expression does not lead to closed form formulas. However, asymptotic expansions are possible, with a particular form depending on the values of x and of $A(\alpha,\theta)$. The main variations of $A(\alpha,\theta)$ are induced by the parameter α, the angle θ being important for small values of α (see Fig. 7). We will therefore consider the following three cases:

- Case $x < 1/2$. Here $\pi x < A(\alpha,\theta)$ in the whole domain D, so that the function under the integral can be expanded in absolutely convergent series in the variable $\pi x/A(\alpha,\theta)$. After integration, the function $f(x)$ can be approximated by

$$f(x) \approx \sum_{p=0}^{K} (-\pi x)^p (p+1) F_p\,, \tag{32}$$

  with K large. The coefficients F_p are given by

$$F_p = \int_0^\pi d\theta \int_0^\infty \frac{ada}{A(a,\theta)^{p+2}}. \tag{33}$$

  As shown in *ftp://ftp.stams.strath.ac.uk/~/pub/sergei/Vcells.xls*, $K = 43$ that gives a reasonable accuracy.

- Case $1/2 < x < 4$. We split the integration domain into two sub-domains: $D_1 = [2,\infty) \times [0,\pi]$ and $D \setminus D_1$. The inequality $\pi x < A(\alpha,\theta)$ still holds in domain D_1 and the same expansion as above gives an expression similar to (32), with coefficients G_p, which are now integrals over D_1 given by

$$G_p = \int_0^\pi d\theta \int_2^\infty \frac{ada}{A(a,\theta)^{p+2}}. \tag{34}$$

More elaborate methods should be used in the domain $D \setminus D_1$ where neither a reasonably fast convergent expansion in $\pi x/A(\alpha,\theta)$ nor that in $A(\alpha,\theta)/(\pi x)$ are possible. In this case we expand the function $A(\alpha,\theta)$ in the variable α at a point α_0 which depends on the range of α. The first term of the expansion, $A(\alpha_0,\theta)$, is then written as $a_1 + a_2(\theta)$ where we take

1. $\alpha_0 = 0$ and $a_1 = 1$ for $\alpha \in [0, 1/4)$;
2. $\alpha_0 = 1/2$ and $a_1 = 11/8$ for $\alpha \in [1/4, 1)$; and finally
3. $\alpha_0 = 3/2$ and $a_1 = 17/4$ for $\alpha \in [1, 2)$.

Denoting all the subsequent expansion terms by a_i $(i = 3, 4, \dots)$ we may now integrate term by term the following expansion of the integration function:

$$\begin{aligned}&\frac{1}{(\pi x + a_1 + \cdots + a_i)^2}\\ &= \sum_{n_2,\dots,n_i=0}^{\infty} (-1)^{n_2+n_3+\cdots+n_i} \frac{(n_2+n_3+\cdots+n_i+1)!}{n_2!n_3!\dots n_i!} \frac{a_2^{n_2} a_3^{n_3} \dots a_i^{n_i}}{(\pi x + a_1)^{n_2+n_3+\cdots+n_i+2}}\,, \qquad (35)\end{aligned}$$

which is absolutely convergent provided all the ratios

$$r_p = \frac{|a_p|}{|\pi x + a_1 + \cdots + a_{p-1}|}, \quad p = 2, \dots, i$$

are less than 1, that is indeed the case. We actually choose α_0 so as to minimize r_1, which optimizes the speed of convergence of the expansion.

This allows us to obtain the following approximation formula for $f(x)$ with complementary terms corresponding to the integration over D_1:

$$\begin{aligned}f(x) \approx &\sum_{p=0}^{K} (-\pi x)^p (p+1) G_p\\ &+ \sum_{p=2}^{6} (-1)^p \left[\frac{c_p^{(1)}}{(1+x)^p} + \frac{c_p^{(3)}}{(17+4x)^p} \right] + \sum_{p=2}^{13} (-1)^p \left[\frac{c_p^{(2)}}{(11+8x)^p} \right], \qquad (36)\end{aligned}$$

where the coefficients $c_p^{(i)}$ are given in Table 2.

- Finally, if $x > 4$ then the integration domain is split into $D_2 = [0,1] \times [0,\pi]$ and $D \setminus D_2$. In D_2 we have $A(\alpha,\theta) < \pi x$ and the expansion is obtained in the variable $A(\alpha,\theta)/\pi x$ with coefficients H_p equal to

$$H_p = \int_0^{\pi} d\theta \int_0^1 a A(a,\theta)^p da. \qquad (37)$$

In $D \setminus D_2$, the same method as in $D \setminus D_1$ allows us to obtain the following expansion

$$f(x) \approx \frac{1}{(\pi x)^2} \sum_{p=0}^{K} \frac{p+1}{(-\pi x)^p} H_p + \frac{5}{24\pi^3 x^4} \ln\left(1 + \frac{1}{x}\right) + \frac{1}{\sqrt{x}} \sum_{p=1}^{3} \frac{d_p}{x^p} + \frac{1}{2\pi(1+x)} + \frac{P_1(x)}{(1+x)^3} + \frac{P_2(x)}{x(1+x)^5} + \frac{P_3(x)}{x^3(1+x)^7}, \quad (38)$$

where

$$P_1(x) = \frac{(15-\pi^2)x - 3\pi^2}{12\pi^3};$$

$$P_2(x) = -\frac{77x^3}{64\pi^5} + \frac{1564x^3 + 4017x^2 + 3970x + 1024}{144\pi^3} + \frac{93x^3 + 195x^2 + 120x}{180\pi};$$

$$P_3(x) = \frac{1}{\pi^{10}} \sum_{j=0}^{6} q_j x^j;$$

with d_p and q_j given in Table 3.

Figure 8 shows the curve (dotted) obtained by the above series expansions. In the intervals $x \in [0.43, 0.5]$ and $[3.66, 5.41]$ the series converge too slowly to be practically useful. The proposed interpolation formulae for $f(x)$ are

$$f(x) \approx \begin{cases} 1.0143 - 0.6566x & \text{for } x \in [0.43, 0.5]; \\ 0.4095 - 0.08076x + 0.00564x^2 & \text{for } x \in [3.66, 5.41]. \end{cases}$$

In the limiting case as x vanishes, the Π_1-cells are rather larger than Π_2-cells so that $\dot{\mathcal{C}}$ almost always coincides with the Π_2 cell containing the origin. Its area is known to be $1.28017/\nu_2$. If $x \to \infty$, the cell $\dot{\mathcal{C}}$ almost coincides with the Π_1 cell centered at the origin, which is known to have for mean area $1/\nu_1$. Accordingly, the asymptotic expansion $1/\nu_2(1+x)$ has the limit $1/\nu_1$.

5.2 Expectation of the area of $\dot{\mathcal{C}}$ with respect to P

Equation (27) is symmetric in ν_1 and ν_2 and will be considered only for values of $x = \nu_1/\nu_2 \geq 1$. It may be written as

$$\mathbf{E}\,|\dot{\mathcal{C}}| = \frac{8\pi}{\nu_2} x \int_D \alpha g(xA(\alpha,\theta))\, d\alpha d\theta \quad (39)$$

where

$$g(y) = \int_D \frac{\alpha d\alpha d\theta}{(y + A(\alpha,\theta))^3}. \quad (40)$$

The approach used in the previous section to derive expansion (38) for $f(x)$ in the case $x > 4$ is immediately applicable to $g(y)$ in the range $y > 4\pi$. The resulting expression is used in (39) provided that the condition $xA > 4\pi$ is verified (remind that $A \geq \pi/2$, so that this condition is verified for $x > 8$). A simple integration then gives the following expansion for the mean area:

$$\nu_2\,\mathbf{E}\,|\dot{\mathcal{C}}| \approx \frac{2\pi F_0}{x} - \frac{6\sqrt{\pi}M_2}{x^{3/2}} + \frac{2F_1(15+2\pi^2)}{3x^2} + \frac{5M_3(128-45\pi^2)}{18\sqrt{\pi}x^{5/2}}$$
$$+\frac{2\pi F_2}{x^3}\left(\frac{-1155+6920\pi^2+576\pi^4}{640\pi^2} - 3H_1\right) + \frac{7M_4(-61683712+15523200\pi^2-1636875\pi^4)}{405000\pi\sqrt{\pi}x^{7/2}} \tag{41}$$

with coefficients F_p, H_p given above and

$$M_p = \int_0^\pi d\theta \int_0^\infty \frac{\alpha d\alpha}{A(\alpha,\theta)^{p+1/2}}$$

$(M_2 = 0.10163420,\ M_3 = 0.03648602,\ M_4 = 0.01612125)$.

The asymptotic expansion (41) approximates the numerical values with a relative error within 3.6% for $x > 8$. For $1/100 < x < 100$ it may be completed by the function

$$[0.8(1+x) + 0.4929\sqrt{x}]^{-1},$$

which approximates $\nu_2\,\mathbf{E}\,|\dot{\mathcal{C}}|$ with a relative error not exceeding 2% in this range. Note that such an approximation is not consistent for large values of x.

The function $\nu_2\,\mathbf{E}\,|\dot{\mathcal{C}}|$ is shown as solid line in Figure 8.

The same reasoning as at the end of the previous section allows one to obtain the limiting behavior of the function that tends to $1.28017/\nu_2$ when $x \downarrow 0$ and behaves like $1.28017/\nu_2(1+x) = 1.28017/\nu_1$ for large x.

5.3 Expectation of the area of $\dot{\mathcal{C}}$ with respect to $\mathbf{P}_Z^{[1,2]}$

In domain $D = [0,\infty) \times [0,\pi]$, the function $A(\alpha,\theta)$ defined by (23) verifies the following relation:

$$A(\alpha,\theta) + \alpha^2 A(\alpha^{-1},\theta) = 2\pi(1+\alpha^2) + 2\alpha[\sin\theta - (\pi+\theta)\cos\theta] \stackrel{\text{def}}{=} 2\pi m(\alpha,\theta)\,. \tag{42}$$

Using this, it is easy to show that expression (28) is indeed symmetric in ν_1 and ν_2, as expected. It is therefore sufficient to consider the case $x = \nu_1/\nu_2 \leq 1$. Formula (28) can be written as

$$\mathbf{E}_Z^{[1,2]}\,|\dot{\mathcal{C}}| = \frac{2\pi}{\nu_2}\frac{1+x}{(1-x)^2}\,j\left(\frac{2x}{1-x}\right),$$

where

$$j(y) = \iint_D \frac{\alpha d\alpha d\theta}{(A(\alpha,\theta) + \pi y m(\alpha,\theta))^2}, \tag{43}$$

where m is defined in (42), and y is positive. Since $A/m < 4\pi/3$ (resp., $2\pi/3 < A/m$) in domain D, we can derive convergent series expansion for $j(y)$ provided that $y > 4/3$ (resp., $y < 2/3$). We have

$$j(y) = \begin{cases} \sum_{p=1} p(-\pi y)^{p-1} K_p, & \text{if } y < 2/3 \\ \sum_{p=1} p(-\pi y)^{-p-1} L_p, & \text{if } y > 4/3, \end{cases} \tag{44}$$

with coefficients $K_p,\ L_p$ given by

$$\begin{aligned} K_p &= \iint_D \frac{\alpha\, m(\alpha,\theta)^{p-1}}{A(\alpha,\theta)^{p+1}} d\theta d\alpha \\ L_p &= \iint_D \frac{\alpha\, A(\alpha,\theta)^{p-1}}{m(\alpha,\theta)^{p+1}} d\theta d\alpha. \end{aligned}$$

In the limiting cases, as $x \downarrow 0$ ($y \downarrow 0$), the function $\mathbf{E}_Z^{[1,2]}\,|\dot{\mathcal{C}}|$ approaches $1.28017\nu_2^{-1}$ and as $x \to 1$ ($y \to \infty$) it tends to $0.59\nu_2^{-1}$.

Figure 8 shows the corresponding curves (dashed). In the range $x \in [0.15, 0.5]$, the interpolation $1.2465 - 1.2907x + 0.7743x^2$ may be used for $\nu_2\, \mathbf{E}_Z^{[1,2]}\,|\dot{\mathcal{C}}|$. Conversely, in the range $x \in [2, 8]$ interpolation formula is given by $1.2465 - 1.2907/x + 0.7743/x^2$.

Acknowledgements. The authors are grateful to Marc Lebourges for interesting discussions on the problem and to anonymous referee whose remarks allowed us to improve the presentation of the material.

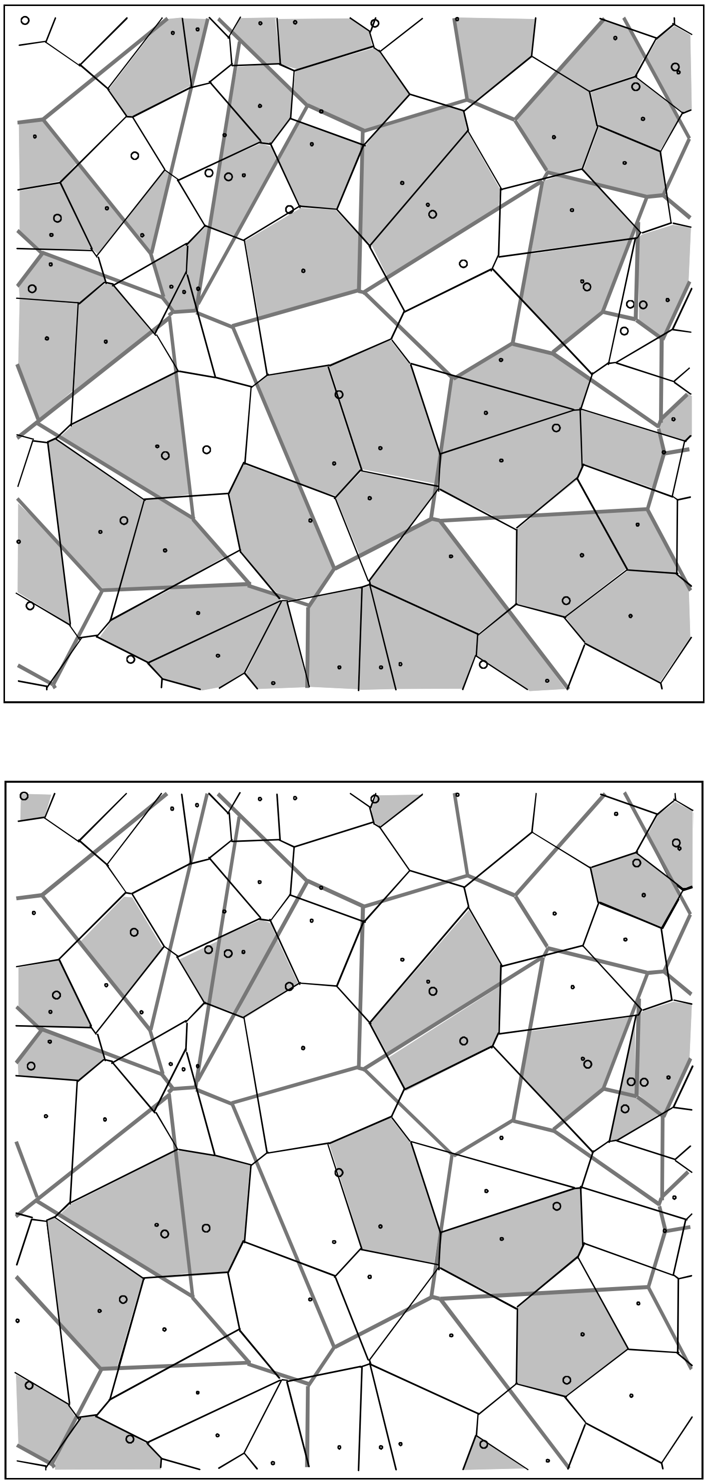

Figure 1: The cells of T containing nuclei of N_1 (top) and N_2 (bottom). Here $\nu_2/\nu_1 = 0.6$. Points of process N_1 are dots, and of process N_2 are circles.

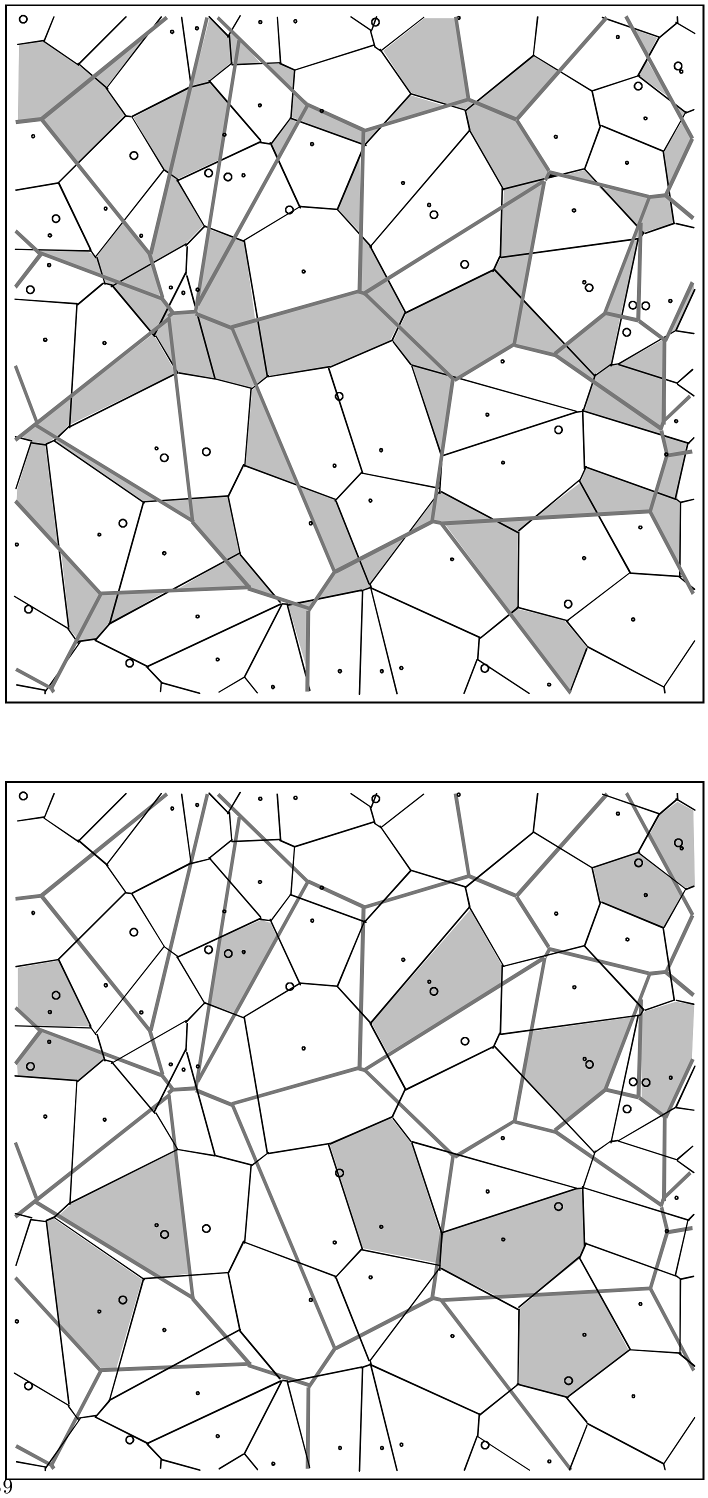

Figure 2: The cells of T containing neither nuclei of N_1 nor N_2 (top) and nuclei of both N_1 and N_2 (bottom).

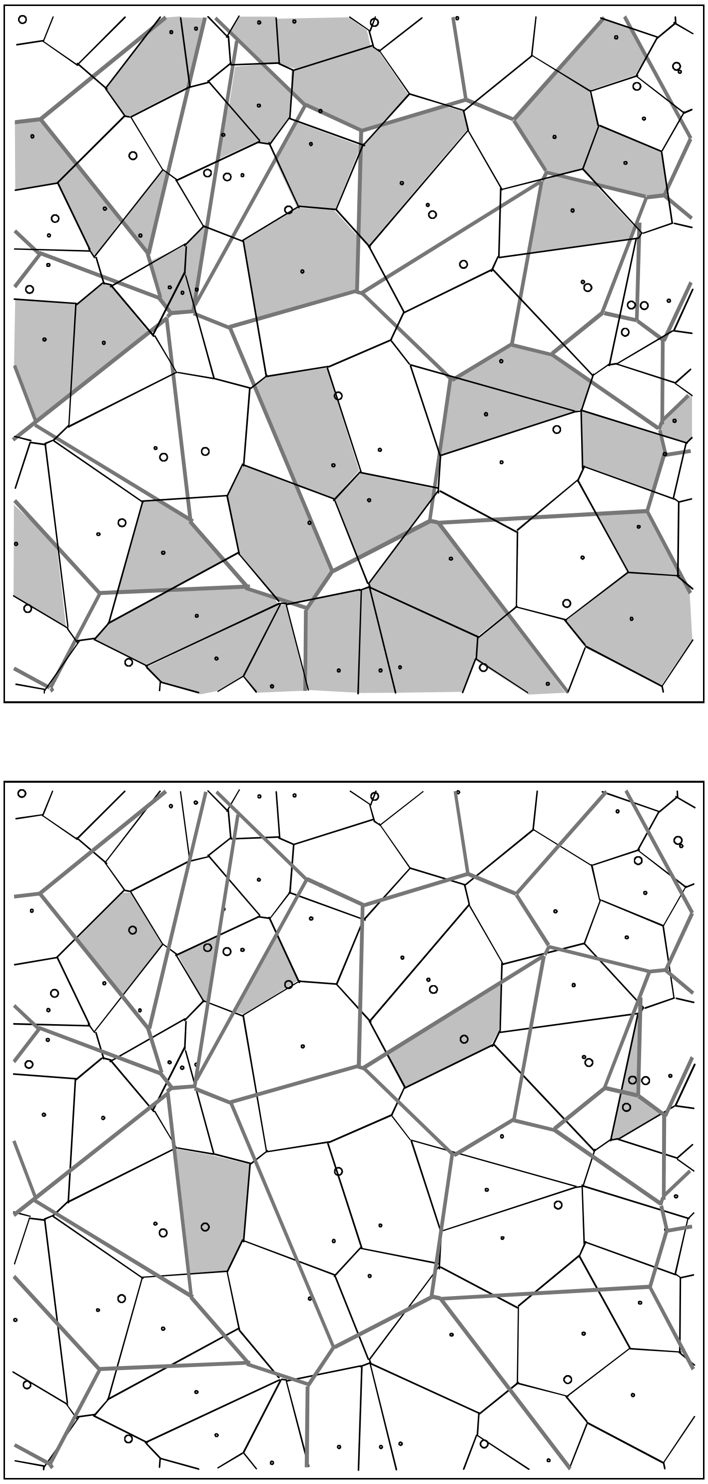

Figure 3: The cells of T containing nuclei of N_1 but not N_2 (top) and nuclei of N_2 but not N_1 (bottom). Note the influence of the ratio ν_2/ν_1 (=0.6 here).

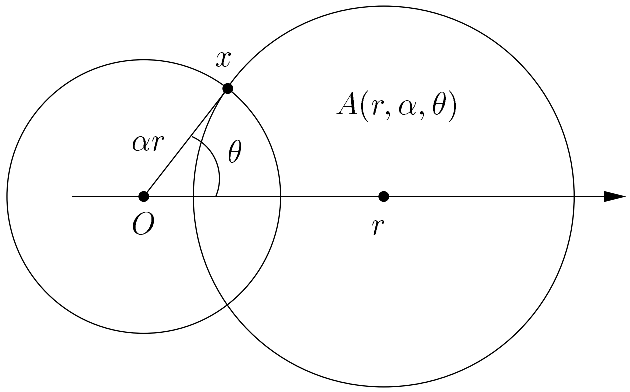

Figure 4: Union of two discs $D_x\big((0,0)\big)$ and $D_x\big((r,0)\big)$.

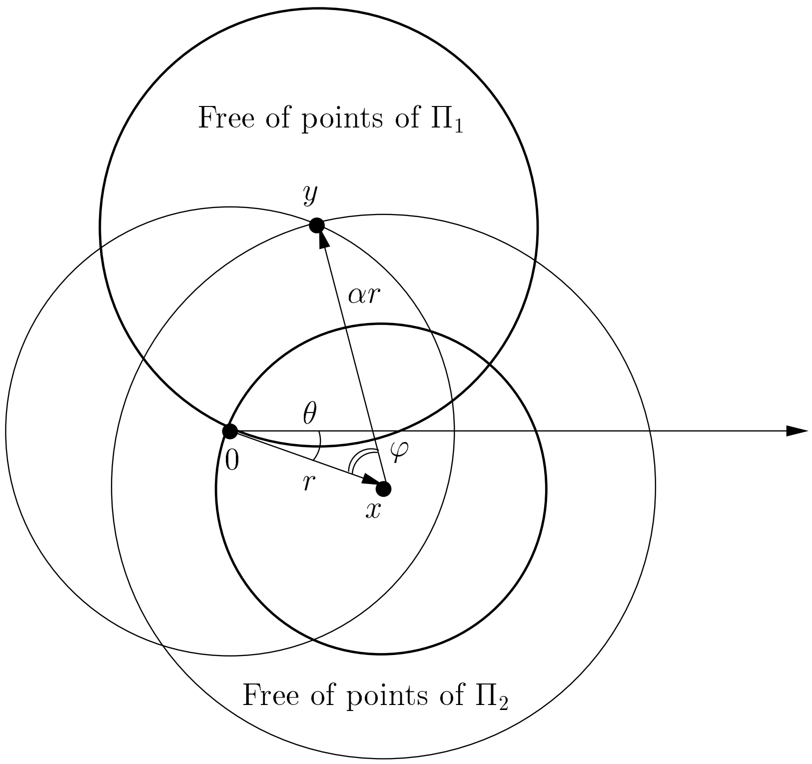

Figure 5:

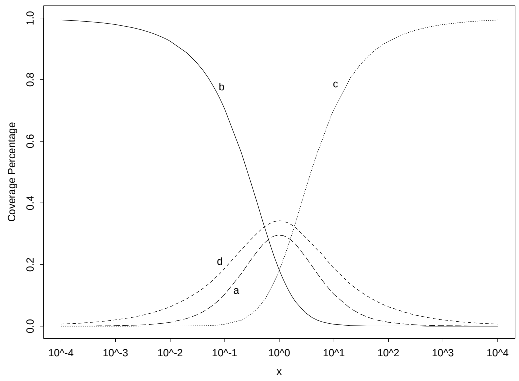

Figure 6: Percentage of the plane covered by the cells containing: a) both Π_1, Π_2-points; b) Π_1 but not Π_2-points; c) Π_2 but not Π_1-points; d) neither Π_1 nor Π_2 points.

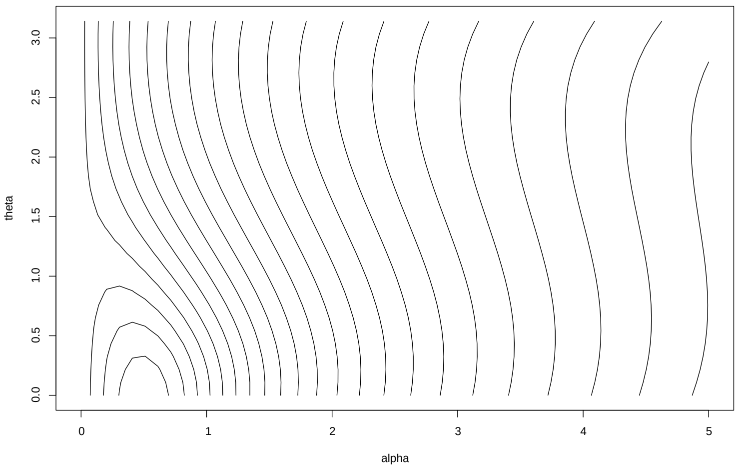

Figure 7: Level lines of function $\log A(\alpha, \theta)$.

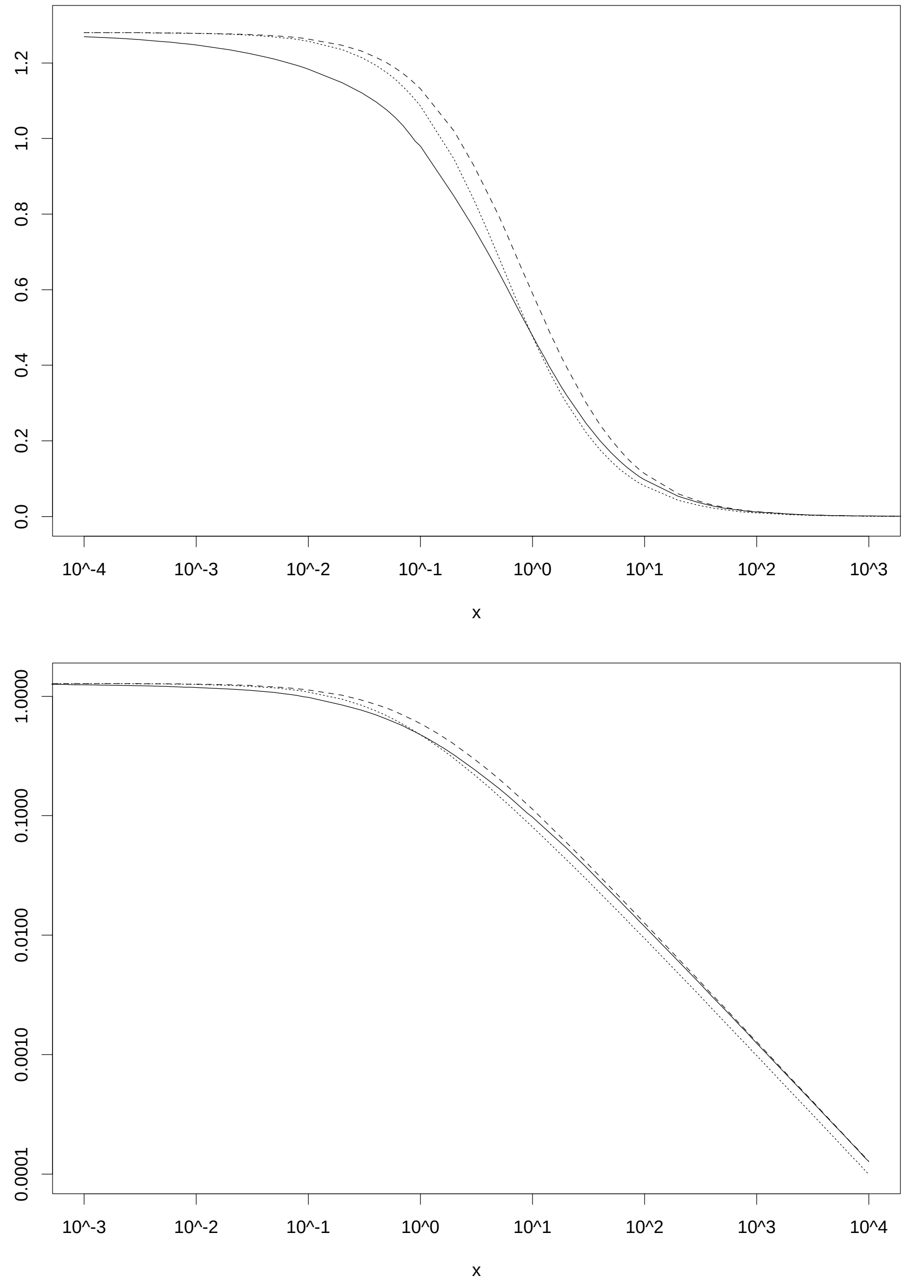

Figure 8: $\nu_2\,\mathbf{E}\,|\dot{\mathcal{C}}|$ – solid line, $\nu_2\,\mathbf{E}_1\,|\dot{\mathcal{C}}|$ – dotted line and $\nu_2\,\mathbf{E}_Z^{[1,2]}\,|\dot{\mathcal{C}}|$ – dashed line, as functions of $x = \nu_1/\nu_2$ (here $\nu_2 = 1$, the lower graph is in log−log-scale).

A Tables

p	$c_p^{(1)}$	$c_p^{(2)}$	$c_p^{(3)}$
2	9.947183943E-03	9.549296586E+00	7.639437268E+00
3	9.325484947E-04	5.887943031E+01	4.416312914E+00
4	1.756649933E-03	1.766497776E+03	1.249007604E+03
5	4.220806849E-04	2.687607506E+04	6.652327703E+03
6	3.811154706E-04	5.464974081E+05	2.795230631E+05
7		9.702580489E+06	
8		1.608492564E+08	
9		2.379754400E+09	
10		3.003362161E+10	
11		2.646874491E+11	
12		1.717633424E+12	
13		7.320755287E+12	

Table 2: Coefficients of the complementary series for $1/2 < x < 4$.

p	d_p	j	q_j
1	$-1/\pi^2$	0	6.210229028E+03
2	$(32-3\pi^2)/(9\pi^4)$	1	2.965870652E+04
3	1.165163489E-02	2	1.036745314E+05
		3	3.150203056E+05
		4	4.616307398E+05
		5	3.057172592E+05
		6	7.078865674E+04

Table 3: Coefficients of the complementary series for $x > 4$.

References

[1] F. Baccelli, M. Klein, M. Lebourges, and S. Zuyev. Géométrie aléatoire et architecture de réseaux de communications. *Annales des Télécommunications*, 51:158–179, 1996.

[2] F. Baccelli, M. Klein, M. Lebourges, and S. Zuyev. Stochastic geometry and architecture of communication networks. *J. Telecommunication Systems*, 7:209–227, 1997.

[3] D. J. Daley and D. Vere-Jones. *An Introduction to the Theory of Point Processes.* Springer, New York, 1988.

[4] G. Grahovac and M. Lebourges. A stochastic geometry model of civil engineering infrastructure in the local loop. In *Proceedings of Networks'96 conference*, Sydney, Australia, 24-29 November 1996.

[5] G. Matheron. *Random Sets and Integral Geometry.* Wiley, New York, 1975.

[6] J. Mecke. *Combinatorial principles in stochastic geometry*, chapter Palm methods for stationary random mosaics, pages 124–132. Armenian Academy of Sciences Publ., 1980.

[7] J. Mecke. Formulas for stationary planar fiber processes III – intersection with fibre systems. *Math. Operations f. Statist., Ser. Statistics*, 12:201–210, 1981.

[8] J. Mecke. On the relationship between the 0-cell and the typical cell of a stationary random tessellation. *Math. Operationsforsch. Statist., Ser. Statistics*, 12(2):201–210, 1998.

[9] J. Møller. *Lectures on random Voronoi tesselations*, volume 87 of *Lect. Notes in Statist.* Springer-Verlag, 1994.

[10] J. Neveu. Sur les mesures de Palm de deux processus ponctuels stationnaires. *Z. Wahrsch. verw. Gebiete*, 34:199–203, 1976.

[11] L. A. Santaló. Mixed random mosaics. *Math. Nachr.*, 117:129–133, 1984.

[12] D. Stoyan, W.S. Kendall, and J. Mecke. *Stochastic Geometry and its Applications.* Wiley series in probability and mathematical statistics. Wiley, Chichester, second edition edition, 1995.

Unité de recherche INRIA Sophia Antipolis
2004, route des Lucioles - B.P. 93 - 06902 Sophia Antipolis Cedex (France)

Unité de recherche INRIA Lorraine : Technopôle de Nancy-Brabois - Campus scientifique
615, rue du Jardin Botanique - B.P. 101 - 54602 Villers lès Nancy Cedex (France)
Unité de recherche INRIA Rennes : IRISA, Campus universitaire de Beaulieu - 35042 Rennes Cedex (France)
Unité de recherche INRIA Rhône-Alpes : 655, avenue de l'Europe - 38330 Montbonnot St Martin (France)
Unité de recherche INRIA Rocquencourt : Domaine de Voluceau - Rocquencourt - B.P. 105 - 78153 Le Chesnay Cedex (France)

Éditeur
INRIA - Domaine de Voluceau - Rocquencourt, B.P. 105 - 78153 Le Chesnay Cedex (France)
http://www.inria.fr
ISSN 0249-6399